

The Respiratory Mechanics of the Yacare Caiman (*Caiman yacare* Daudine)

Michelle N. Reichert¹, Paulo R.C. de Oliveira^{2,3}, George M.P.R. Souza⁴, Henriette G. Moranza⁵, Wilmer A.Z. Restan⁵, Augusto S. Abe⁶, Wilfried Klein², William K. Milsom⁷

¹Royal Veterinary College, University of London, London, UK

²Faculdade de Filosofia, Ciências e Letras de Ribeirão Preto, Universidade de São Paulo, Ribeirão Preto, SP, Brazil

³Instituto Federal do Paraná- Câmpus Avançado Goioerê, Goioerê, PR, Brazil

⁴School of Medicine of Ribeirão Preto, Universidade de São Paulo, Ribeirão Preto, SP, Brazil

⁵Clinica Médica Veterinária, Universidade Estadual Paulista, Jaboticabal, SP, Brazil

⁶Departamento de Zoologia, Universidade Estadual Paulista, Rio Claro, SP, Brazil

⁷Department of Zoology, University of British Columbia, Vancouver, B.C., Canada

Author for correspondence: Michelle N Reichert, mreichert4@rvc.ac.uk

Key words: respiratory mechanics, static compliance, dynamic compliance, elastic forces, resistive forces, work of breathing

Summary Statement: The respiratory system of the caiman stiffens during development as the body wall becomes more muscular and keratinized. Most of the work of breathing is required to overcome elastic forces and increases when animals are submerged. Flow resistance, primarily arising from the lungs, plays a significant role at higher ventilation frequencies.

Abstract

The structure and function of crocodilian lungs are unique compared to other reptiles. We examine the extent to which this, and the semi-aquatic lifestyle of crocodilians affect their respiratory mechanics. We measured changes in intratracheal pressure in adult and juvenile caiman (*Caiman yacare*) during static and dynamic lung volume changes. Respiratory mechanics of juvenile caiman were additionally measured while floating in water and submerged at 30°, 60°, and 90° to the water's surface. The static compliance of the juvenile pulmonary system (2.89 ± 0.22 mL cmH₂O 100g⁻¹) was greater than that of adults (1.2 ± 0.41 ml cmH₂O 100g⁻¹), suggesting that the system stiffens as the body wall becomes more muscular and keratinized in adults. For both age groups, the lungs were much more compliant than the body wall, offering little resistance to air flow (15.35 and 4.25 for lungs, versus 3.39 and 1.67 mL cmH₂O 100g⁻¹ for body wall, in juveniles and adults respectively). Whole system dynamic mechanics decreased with increasing ventilation frequency (f_R), but was unaffected by changes in tidal volume (V_T). The vast majority of work of breathing was required to overcome elastic forces, however work to overcome resistive forces increased proportionally with f_R . Work of breathing was higher in juvenile caiman submerged in water at 90°, due to an increase in work to overcome both elastic and flow resistive forces. The lowest power of breathing was found to occur at high f_R and low V_T for any given minute ventilation (\dot{V}_E) in caiman of all ages.

Introduction

In all reptiles, respiratory movements are powered by axial muscles of the thorax and/or abdomen (Gaunt and Gans, 1969; Rosenberg 1973, Carrier, 1987, 1990; Farmer and Carrier, 2000). The forces that these muscles must generate to produce breathing movements are required to overcome elastic and flow resistive forces associated with expanding and compressing the body wall and lungs. In no other vertebrate group than in the reptiles, are there such wide differences in the structure of both the lungs and body wall (Perry et al., 2005), as well as in the internal divisions of the body cavity (Klein and Owerkowicz, 2006). Lung structure in reptiles ranges from the simple edicular lungs of some lizards to the multicameral, bulliform lungs of the crocodilians (Perry, 1998). Despite this diversity, the lungs of reptiles in general are very compliant and most of the work of breathing is required to expand the body wall (Milsom & Vitalis, 1984; Bartlett et al., 1986). The body wall of reptiles ranges from the relatively compliant chest of some lizards to the heavily armoured chest walls of crocodilians and chelonians.

Although the lungs of Crocodylia are amongst the more complex, the static lung compliance of the Nile crocodile lies in the middle of the range reported for reptiles at 4.32 ml/cm H₂O/ml V_{LR} (Perry, 1988). And while their body walls are amongst the most heavily armored, their static body wall compliance is 0.85 ml/cm H₂O/ml V_{LR} (Perry, 1988), similar to values reported for lizards (Perry and Dunker, 1978). While these values would suggest that most of the work of breathing in the Crocodylia would be required to expand the body wall, as in other reptiles, these measures of static respiratory mechanics only provide information about the work required to overcome elastic forces under resting conditions. They do not address the changes that occur during ventilation when compliance decreases with dynamic movement and when work must also be done to overcome flow resistive forces in both the lungs and chest wall. Several factors, including lung morphology, the respiratory pumping mechanism, and habitat, suggest that the story may be more complex.

Recent research supports early suggestions that much of the lung of crocodylians may be relatively rigid and that airflow through the lung may be unidirectional, flowing posterior in the cervical ventral bronchus and its branches and anterior in the dorsobronchi and their branches during both lung inflation and deflation (Farmer, 2015). Claessens (2009), on the other hand, has shown that the lungs of *A. mississippiensis* may undergo large volume changes between maximal inspiration and expiration.

The respiratory pump is also unique in crocodylians. The diaphragmaticus muscle, which originates on the pelvis and caudoventral body wall and inserts on the lateral and ventral portions of the liver capsule, affects inspiration by retracting the liver, displacing the lungs caudally while both the external and internal intercostal muscles contract simultaneously during inspiration in *Caiman crocodylus* stiffening, rather than expanding the body wall (Gans and Clark, 1976). Recently it has been shown that the diaphragmaticus muscle plays an important role as a locomotor muscle during diving in the American alligator (Uriona and Farmer, 2008; Uriona et al., 2009), whereas its function as a ventilatory muscle becomes only significant in *C. porosus* during treadmill exercise (Munns et al., 2012). In fasting *A. mississippiensis* the diaphragmaticus muscle is also not important for maintaining vital capacity (Uriona and Farmer, 2006). Active expiration is produced by contraction of the transversus abdominis muscle, reducing the volume of the abdominal cavity and forcing the liver cranially (Gans and Clark, 1976; Farmer and Carrier, 2000). Finally, in nature, crocodylians spend the majority of their time floating on, or submerged to varying degrees in water. While submergence of humans in water has been found to significantly increase work of breathing (Hong et al., 1969), it may allow crocodylians floating parallel to the water's surface to expand the chest without having to lift their mass as may be necessary while lying sternally on land. Many crocodiles also breathe at the surface with their bodies submerged to varying degrees and it has been shown that this leads to passive expiration with inspiration requiring increased muscular activity (Gans and Clark, 1976).

Determining the effects of these unique features of lung morphology, respiratory pumping, and habitat, on pulmonary mechanics in crocodylians, requires measures of the changes in dynamic compliance and resistance at physiological breathing frequencies and tidal volumes. The aim of the present study, therefore, was to measure the static and dynamic pulmonary mechanics of the caiman, *Caiman yacare* to determine how the architecture of crocodylian lungs, the armour of the body wall and the influence of land, water, and submersion to different depths is reflected in the mechanics of the respiratory system.

Materials and Methods

Animals

Six caiman (*Caiman yacare*; 39.4 ± 2.2 g) were born and raised in Rio Claro, SP, Brazil at the Universidade Estadual Paulista and entered the study at 5 months old (which the authors consider a juvenile age/life stage). Animals were kept in groups with free access to pools. Four other caiman were transported to Vancouver, Canada from Brazil as juveniles and raised at the animal care centre at the University of British Columbia. Animals were raised in pairs with free access to pools. The adult caiman weighed 27.9 ± 3.2 kg at the time of the experiments. All experimental procedures were performed according to UBC Animal Care Committee protocol A13-0125 under the guidelines of the Canadian Council on Animal Care.

Instrumentation

Adult caiman were immobilized and given 10mg/kg telazol before being intubated and manually ventilated with air and 1.5% isoflurane. Telazol is an NMDA receptor inhibitor similar to ketamine used for induction of general anesthesia followed by an inhalent anesthetic. Juvenile caiman were overdosed with urethane via IP injection, then a tracheal cannula was inserted. A pressure transducer attached to the intubation tube/tracheal cannula via a side arm was used to measure intratracheal pressure.

Experimental Protocol

To produce static pressure-volume curves the anaesthetized individuals were placed in a prone position and inflated and deflated three times, then allowed to return to resting lung volume and pressure. From rest, room air was added to the lungs in a step-wise fashion using a syringe, in 200mL increments for adults and 0.5mL increments for juveniles. Inflations ceased when intratracheal pressures reached approximately 30 cmH₂O. Lungs were then deflated in the same stepwise fashion, past the resting lung volume until the pressure was approximately -20 cmH₂O, and finally inflated again to resting lung volume. The trachea was then opened to the atmosphere, the lungs were fully inflated, and then allowed to return to resting volume. This procedure was then repeated twice more.

A pneumotachograph and differential pressure transducer (DP103-18; Validyne, Northridge, CA, USA) were then connected between the tracheal tube and a ventilator (Harvard Apparatus) to measure air flow. All signals were amplified, filtered, and recorded on a PowerLab 8/35 data acquisition system (ADInstruments Pty Ltd., Colorado Springs, CO, USA). Flow and intratracheal pressure were measured at tidal volume (V_T) and breathing frequency (f_R) combinations of 200, 400, 600 mL and 10, 15, 20, 25, 30, 35, 40 breaths/minute for adults and 1, 2, 3 mL and 20, 30, 40, 50, 60, 70 breaths/minute for juveniles.

For the juvenile caiman, static and dynamic inflations were repeated in a water bath with their bodies placed at 0°, 30°, 60° and 90° to the surface of the water (Fig. S1). Animals were kept at the appropriate angle in the water column using string and weights, with care being taken not to kink the trachea in a way that would influence pressure readings.

After static and dynamic measurements were completed on the intact animals, the animals were placed in a supine position, their body cavity was opened and all muscle and organs were removed from around the lungs. The experimental protocol was then repeated on the exposed lungs.

Data Analysis and Statistics

Flow curves were integrated to produce volume (ATPD), and pressure-volume loops were generated using LabChart software (ADInstruments). Static lung (C_L) and total system (C_T) compliance were measured as the slope of the static deflation curve at its steepest point. Body wall compliance (C_B) was calculated from these values using the equation:

$$\frac{1}{C_T} = \frac{1}{C_L} + \frac{1}{C_B}$$

Dynamic compliance was measured as the slope of the line connecting the points of zero flow on the pressure-volume loops (the points of maximum and minimum volume). Pressure-volume loops were generated for 10 breaths at each combination of tidal volume and breathing frequency. Dynamic C_B was calculated from dynamic C_T and C_L using the equation above. Work to overcome elastic forces (elastic work) was measured as the area of the triangle made between the two points of zero flow and the coordinate (0, maximum volume)(Fig. S2A). Work to overcome resistive forces (resistive work) was measured as the area enclosed by the compliance line and the curve of the loop during the inflation phase. Total work per breath is the sum of these two work components (elastic and resistive; Otis, 1954). For purposes of conversion, 1 Joule = 1L.cm H₂O. The minute work (or power) of breathing was calculated by multiplying the total work per breath by the breathing frequency.

All data are shown as means \pm 1 SEM. Data are normalized to body weight when adult and juvenile caiman are being directly compared. Data were statistically analyzed using SigmaStat version 3.5 (Systat Software Inc.). A two-way repeated measures ANOVA was used to determine significant differences (defined as $P < 0.05$) between different tidal volumes and over different breathing frequencies. A Holm-Sidak *post hoc* test was used when significant differences were detected by the ANOVA. Statistical comparison of adult and juvenile static compliance means was achieved using a T-test.

Results

Static Mechanics

Figure S3 depicts one representative static pressure-volume curve from an adult (Fig. S3A) and a juvenile (Fig. S3B) caiman. C_L was larger than C_B and C_T for both adults (C_L : 4.25 ± 0.74 , C_B : 1.67 ± 0.92 , C_T : 1.20 ± 0.41 mL cmH₂O⁻¹ 100g⁻¹) and juveniles (C_L : 15.35 ± 0.90 , C_B : 3.39 ± 0.51 , C_T : 2.89 ± 0.22 mL cmH₂O⁻¹ 100g⁻¹). C_T was significantly larger in juveniles (2.89 ± 0.22 mL cmH₂O⁻¹ 100g⁻¹) than in adults (1.20 ± 0.41 mL cmH₂O⁻¹ 100g⁻¹; $P = 0.002$). Because of the tendency of the lungs of the juveniles to rupture upon opening the chest cavity, the sample size for C_L and C_B of juveniles ($N = 2$) was too small to allow statistical comparison with the adults although here too the compliances appear much larger. There was no significant difference between the total compliance at different angles in the water column (0°: 2.11 ± 0.14 , 30°: 2.73 ± 0.21 , 60°: 2.52 ± 0.37 , 90°: 2.90 ± 0.40 mL cmH₂O⁻¹ 100g⁻¹).

Dynamic Mechanics

Pressure-Volume Relationships

Dynamic compliance and work of breathing were determined from pressure-volume loops like the representative loops shown in Figure S2. Dynamic compliance was taken from the slope of the line connecting the two points of zero flow. The area below this line but above the inflation curve (area ABIA on Fig. S2A) was taken as the work to overcome resistive forces. The area above this line but below the horizontal line made between the end-inspiration point on the loop and the y-axis was taken as the work of overcome elastic forces (area ABCA on Fig. S2A). Together, resistive work and elastic work sum to equal the total work of inflation.

Figures S2B and S2C are representative loops from a single adult caiman and illustrate how the pressure-volume relationship changes as V_T or f_R are manipulated in isolation of the other. Pressure increased as V_T increased when f_R was kept constant (Figure S2B) and vice versa when V_T was kept constant (Figure S2C).

Dynamic Compliance

Dynamic compliance decreases as f_R increases in both adults and juveniles ($P < 0.01$; Fig. 1A & B). There is no effect of V_T on dynamic compliance. In juvenile caiman, compliance is greater in water at 0° compared to when they are submerged in water at 90° ($P < 0.02$; Fig. 1C). It tended to be greater than when the animals were positioned prone on land but the difference was not significant.

Dynamic compliance in juvenile caiman was significantly higher for the isolated lung compared to the compliance of the body wall and whole system at low f_R ($P < 0.01$; Fig. 1D-F). As V_T and f_R increased, dynamic compliance of the isolated lung decreased. Due to experimental constraints, the dynamic mechanics of the isolated lung could not be measured in the adult caiman.

Work of Breathing

Total Work

Total work for both adults and juveniles increased with V_T and f_R when the animal was in air (Fig. 2). Figure 5 compares total work across all submergence angles for juvenile caiman. There was little difference in total work at different angles of submergence except at 90° , where total work was often significantly higher ($P < 0.05$; Fig. 3).

Elastic and Resistive Work

Total work was proportionally dominated by elastic work in both adult and juvenile caiman (Fig. 4). There was an increase in the proportion of total work dedicated to resistive work as f_R increased in both adults and juveniles. The increase in total work seen at 90° submergence in juveniles was due to an increase in both elastic and resistive work (Fig. 5).

Minute Ventilation and Power

Figure 8 depicts the relationship between work and minute ventilation (\dot{V}_E) for adults and juveniles. As minute ventilation increased, so did work of breathing and for any given f_R (depicted by the isopleths in Fig. 6). Work was also greater at higher tidal volumes. From this graph, power was found by taking the f_R and V_T combinations that, when multiplied, gave specific values of \dot{V}_E (4000, 6000, 8000 mL/min for adults and 40, 60, 80 mL/min for juveniles) and multiplying the corresponding work values by the corresponding f_R (in seconds⁻¹). This yields power in watts. Power was then plotted against f_R (Fig. 7). For each \dot{V}_E , power decreased initially as f_R increased (Fig. 8) but began to rise again at the highest f_R (and lowest V_T).

Discussion

The aim of the present study was to determine how the architecture of crocodilian lungs, the armour of the body wall and the influence of land, water, and submersion to different depths are reflected in the mechanics of the respiratory system. This study examined the work required to artificially ventilate the respiratory system of caiman and the values obtained may vary from those obtained during spontaneous ventilation. When caiman breathe spontaneously, the muscles of the chest wall and abdomen contract altering the compliance of the thorax and abdomen and, as a consequence, our results may underestimate the true costs of breathing.

We found that the stiffness of the body wall plays a key role in determining the static mechanics of the intact respiratory system. The body wall is significantly less stiff in the juvenile caiman. This likely reflects a combination of increased muscularization, thickening of the skin and development of osteoderms. Osteoderm growth has been shown to initiate at about 1 year in *A. mississippiensis* (Vickaryous and Hall, 2008). This suite of changes during development leads to a large reduction in body wall compliance. There was a further significant reduction in the compliance of the total system going from static conditions (no ventilation) to ventilation,

especially at higher ventilation frequencies. In the juvenile caiman (the only group for which we could partition changes in compliance), this was largely due to a decrease in the compliance of the lungs. Thus, whereas the structure and rigidity of the body wall of the thorax and abdomen largely determined the static pulmonary mechanics of the system, significant effects arise in conjunction with lung architecture when the dynamics of the system are considered. As a result, although the majority of work was required to overcome elastic forces at low pump frequencies, at higher frequencies an increasing proportion of the work is required to overcome flow resistive forces, particularly in the adult caiman. In juveniles, submergence in water reduced dynamic compliance significantly at the steepest flotation angle and at higher pump frequencies, increasing the work required to ventilate the system. Laying at the surface of the water appeared to require less work to overcome elastic forces compared to resting on land, presumably due to the freedom for abdominal expansion provided by flotation, although this was not significant.

Static Mechanics

As has been shown for other reptiles, the static pressure-volume relationship of the intact respiratory system of the caiman (both adult and juvenile) primarily reflects the mechanical properties of the chest wall. The lungs are very compliant and thus the total compliance of the intact respiratory system is almost identical to the compliance of the body wall. Our values for the adult caiman are very similar to those reported previously for the Nile crocodile (Perry, 1988, Table 1). A comparison of compliance values for the total respiratory system, body wall and lungs of various species of reptiles and mammals indicates that the respiratory system of crocodylians is relatively stiff, similar to that of the turtle (Table 1). The relatively stiff respiratory system of the turtle has been attributed to the animal's shell (Vitalis and Milsom, 1986) and that of the crocodylians most likely reflects their thick skin and dense body armour when older. The values obtained for the juvenile caiman are roughly twice those of the adult crocodylians, most likely reflecting a lack

of osteoderms and a lower degree of muscle mass and keratinization of the body wall. Of note, however, is that the compliance values normalized to body weight show that adult crocodylians still possess a more compliant system than mammals; the C_T for crocodylians is roughly 6 times greater than the C_T for most mammals (Table 1). The low compliance of the respiratory system of mammals, however reflects the low compliance of the lungs, as well as that of the body wall (Table 1). Comparisons made on a volume basis (compliance normalized to the volume of the lung in vivo when open to atmosphere (V_{LR})), however, show that the total system compliance of the crocodylians is quite similar to that of the various lizard species and 4 to 7 times more compliant than that of the turtle (Table 2). This suggests that the relatively small size of the relaxed respiratory system of crocodylians also contributes to their low C_T . The V_{LR} of the crocodylians is only 13-15% of their total lung volume (V_L or vital capacity (VC)) whereas that of other reptiles is in the range of 20-36% (Perry and Dunker 1978, Table 2).

While these values would suggest that most of the work of breathing in Crocodylia would be required to expand the body wall, as in other reptiles, these measures of static respiratory mechanics only provide information about the work required to overcome elastic forces under resting conditions.

Dynamic Mechanics

The dynamic compliance (C_{dyn}) of the respiratory system, in both juvenile and adult caiman, was highly frequency dependent. The system became stiffer as frequency increased. The decrease in compliance with increasing frequency, in the juveniles at least, was largely due to a reduction in the compliance of the lungs (Fig. 1). The decrease in compliance going from static conditions (no ventilation) to ventilation at the lowest pump frequencies used in this study (3 seconds/cycle or simulated breath) was dramatic. The static compliance of the total system in the caiman was roughly three to five times greater than the dynamic compliance for adult and juvenile caiman at the lowest pump frequencies, respectively. Similar results have been reported for geckos (Milsom & Vitalis, 1984) and turtles (Vitalis and Milsom, 1986). The total system compliance, however, was unaffected by

changes in V_T over the range studied. Thus, whereas the structure and rigidity of the body wall of the thorax and abdomen largely determined the static pulmonary mechanics of the system, significant effects arise in conjunction with lung architecture when the dynamics of the system are considered. This is similar to the results reported for turtles (Vitalis and Milsom, 1986) but not geckos where C_{dyn} decreased with increasing pump volume at high ventilation frequencies (Milsom and Vitalis, 1984).

The dependence of C_{dyn} on frequency observed in the caiman means that a greater change in pressure will result for any given change in volume as frequency increases (or that a greater change in pressure will be required to produce the same volume change at higher frequencies). This is reflected in the measurements of the total work obtained for the total respiratory system (Fig. 2) particularly in the adults. Work per breath increases exponentially with increases in volume for any given ventilation frequency. Likewise, the work per breath increases with increasing frequency for any given pump volume, corresponding with a smaller slope of the rise in W at low frequencies but a larger slope at higher pump frequencies. This increase in work is primarily due to an increase in the work needed to overcome non-elastic forces (Fig. 4). Therefore, at low pump frequencies most of the work is required to overcome elastic forces and at higher frequencies an increasing proportion of the work is required to overcome flow resistive forces, particularly in the adult caiman. In adults, the work required to overcome elastic forces accounted for approximately 70% of the total work at low pump volumes, decreasing to 50% at the highest pump frequencies. For juveniles the work required to overcome elastic forces accounted for approximately 80% and 70% of the total work at low and high pump frequencies, respectively. We could not partition this increase in flow resistance to changes in the lung versus the body wall but it is likely both contribute to some extent.

In comparison, Tokay geckos require almost the entirety of their total work of breathing to be devoted to overcoming elastic forces (Milsom & Vitalis, 1984). In turtles, respiratory work is divided equally between overcoming elastic and non-elastic forces at lower frequencies and volumes. At high frequencies and tidal volumes, however, the work required to overcome non-elastic forces dominates total work (Vitalis and Milsom, 1986). In mammals, respiratory work primarily overcomes elastic forces at low pump frequencies and non-elastic forces at high pump frequencies (Otis et al. 1950).

The role of body wall compliance in crocodilian breathing mechanics was questioned previously because of the unique breathing mechanism found in crocodilians. Gans & Clark (1976) reported that in *Caiman crocodilus* both external and internal intercostal muscles contracted simultaneously during ventilation, stiffening the body wall. A separate muscle, the diaphragmaticus, acts as a hepatic piston pump, retracting the liver and displacing the lungs caudally, which contributes significantly to lung ventilation, at least during exercise (Munns et al., 2012), but not to vital capacity (Uriona and Farmer, 2006). Furthermore, abdominal muscles, gastralia and pelvic rotation aid in crocodilian ventilation (Carrier and Farmer, 2000). The net result is expansion of the abdomen rather than the thorax. In the present study with pump ventilation, we do not distinguish between thorax and abdomen and treat the body wall as a single element. Clearly expansion will occur at the most compliant portion of the body cavity.

Figure 6 shows clearly that increasing tidal volume is a more expensive strategy for increasing ventilation than increasing breathing frequency. Increasing tidal volume over breathing frequency, however, reduces the proportion of dead space ventilation, and is a more effective strategy for O₂ uptake. Therefore, the relative benefits of a deeper breathing pattern depend on whether improvements in pulmonary O₂ uptake outweigh the added metabolic costs associated with the work of breathing. The greater the dead space volume, the greater the advantage of preferentially increasing tidal volume.

In both juveniles and adults, the work required to ventilate the system at any given level of \dot{V}_E , was greater for slow deep breaths than for fast shallow breaths (Fig. 8). When dead space ventilation was taken into account, the power (minute work) required for ventilating the system at a constant level of \dot{V}_{eff} (where $V_{eff} = V_T - V_D$ and V_D = the dead space of the trachea and primary bronchi, estimated to be 3ml/kg (Sanders and Farmer, 2012)) is a product of the work per breath multiplied by the f_R , or pump frequency. The combination of f_R and V_{eff} which produces minimal work of ventilation can be determined from a power curve when power is expressed as a function of f_R for constant levels of \dot{V}_{eff} . When f_R is below this optimal combination, minute work increases with increasing V_{eff} , in order to overcome increases in elastic forces in the body wall. When f_R is above this level, increases in minute work are primarily to overcome increases in non-elastic (flow-resistive) forces in the lung.

Water submergence

We have often observed that when caiman (juvenile and adult) first approach the water surface, they do so at a steep angle and can hang in the water with their bodies 60 to 90 degrees to the surface (Fig. S4). If they remain at the surface for any length of time, in most cases their bodies will come to lie parallel to the surface. The ability of crocodylians to shift their centre of buoyancy with respect to centre of mass to control posture, pitch and roll has been well described (Uriona and Farmer, 2006). The diaphragmaticus and ischiopubis muscles move the lung ventrocaudal during ventilation and it is thought that these muscles are also used to change pitch by shifting the relative buoyancy of the caudal versus cranial portions of the body (Uriona and Farmer, 2006).

In juveniles, while water immersion had no effect on the static compliance of the intact system, it reduced dynamic compliance significantly particularly at the steepest flotation angle, where the lowest point of the lungs was at a hydrostatic pressure of about 5 cmH₂O, and at higher pump frequencies. As a result, it increased

the work required to ventilate the system under these conditions. Surprisingly this was due to an increase in the work required to overcome flow resistive forces, which could be associated with the lung, chest wall or both. There was a nonsignificant trend for the work required to overcome elastic forces to be less while floating at the water's surface compared to resting on land, presumably due to the freedom for abdominal expansion provided by flotation.

We were unable to run the water submergence protocol on the larger caiman. Due to their larger size, their lungs would be further below the water surface at any given flotation angle compared to the juveniles and thus the effects of water submergence are likely to be greater. This remains to be determined.

Perspective:

In general, when breathing room air, caiman breathe episodically (Tattersall et al. 2006) as has been described for other crocodylians (Naifeh et al. 1970, 1971; Glass and Johansen 1979; Zhao-Xian et al. 1991; Douse and Mitchell 1992a; Hicks and White 1992; Munns et al. 1998). While absolute breathing frequency is quite low, the rates of air flow during active inspiration and expiration can be quite high. From a mechanical perspective, the key timing components are the time spent inspiring and expiring and hence the instantaneous breathing frequency ($60 \text{ seconds} / T_{\text{tot}}$ (the length of the active breath in seconds)). We can use values taken from the literature for instantaneous breathing frequency in various crocodylians (Table S1) to determine the work per single breath and the power required for continuous breathing. These results can be used to determine whether breathing patterns in crocodylians naturally minimize the cost of ventilation. It has been suggested that in animals taking single breaths, work per breath is most useful for assessing the mechanical efficiency of breathing. In comparison, minute work (power) is used to measure efficiency in animals that breath continuously (Milsom, 1984).

Fig. 8 shows the mechanical cost of a single breath at various V_T as a function of the instantaneous frequency ($60/T_{TOT}$). These work-per-breath curves illustrate the rates at which work increases as either the volume of a breath or the frequency at which the breath is taken increase. Clearly it is less expensive to take small slow breaths. The values of V_T and f_R for intact crocodilians spontaneously breathing various gas mixtures (Table S1) are placed on the graph for comparison. The position of the breaths measured in spontaneously breathing animals on the work-per-breath curve represent a compromise between mechanical and biological constraints. A low V_T compromises alveolar ventilation and gas exchange. The need to keep V_T sufficiently large in order to overcome dead space and maintain gas exchange, on the one hand, and the increased mechanical work associated with increases in V_T , on the other, undoubtedly interact to produce the resting level of V_T . Given low metabolic rates and low levels of total ventilation, there are fewer constraints on rates of inspiration and expiration and all crocodilians inhale and exhale relatively slowly (low instantaneous breathing frequencies (Table S1)).

The power required to maintain different constant levels of alveolar ventilation are plotted as a function of pump frequency (f_R) in the lower graph of Fig. 8. The range of combinations of f_R and V_T measured in different species of spontaneously breathing crocodilians is superimposed on these curves. It can be seen that the f_R of spontaneously breathing animals is much lower than the pump frequencies associated with the minimum power to maintain a constant level of effective ventilation. These higher frequencies and much lower levels of V_T at which the power required for air movement are minimal, however, may reflect the mechanics of gular flutter seen in heat stressed animals (Naifeh et al., 1970; Munns et al., 2012) where small volumes are moved rapidly in and out utilizing the respiratory dead space for thermal cooling without producing respiratory alkalosis (Video S6).

Acknowledgements

This work was supported by a discovery grant to WKM from the Natural Sciences and Engineering Research Council (NSERC) of Canada, and grants from Brazil from the Instituto Nacional de Ciência e Tecnologia em Fisiologia Comparada (Fundação de Amparo à Pesquisa do Estado de São Paulo (FAPESP, n° 2008/57712-4), Conselho Nacional de Desenvolvimento Tecnológico e Científico (CNPq, n° 573921/2008-3)), Coordenação de Aperfeiçoamento de Pessoal de Nível Superior (CAPES), and Universidade Estadual Paulista (UNESP). This project was completed as a part of the IVth International Course on Comparative Physiology of Respiration held at Sao Paulo State University in Jaboticabal, Brazil. We are grateful to everyone involved in the organization and execution of the program.

The authors declare no competing interests.

Author contributions

Conceptualization, methodology, project administration: W.K.M. and WK; Data collection: everyone; Formal analysis: MNR with the assistance of everyone; Writing - original draft preparation: MNR. Funding acquisition: W.K.M., WK.

Literature Cited

- Bartlett, D., Mortola, J.P., and Doll, E.J.** (1986). Respiratory mechanics and control of the ventilatory cycle in the garter snake. *Respiration Physiology*. **64**, 13-27.
- Bennett, F.M., and Tenney, S.M.** (1982). Comparative mechanics of mammalian respiratory system. *Respiration Physiology*. **49**, 131-140.
- Carrier, D.R.** (1987). Lung ventilation during walking and running in four species of lizards. *Exp. Biol.* **47**, 33-42.
- Carrier, D.R.** (1990). Activity of the hypaxial muscles during walking in the lizard *Iguana iguana*. *J. Exp. Biol.* **152**, 453-470.
- Carrier, D.R., Farmer, C.G.** (2000). The integration of ventilation and locomotion in archosaurs. *Amer. Zool.* **40**, 87-100.
- Claessens, L.P.A.M.** (2009). A cineradiographic study of lung ventilation in *Alligator mississippiensis*. *J. Exp. Zool.* **311A**, 563-585.
- Crossfill, M.L. and Widdicombe, J.G.** (1961). Physical characteristics of the chest and lungs and the work of breathing in different mammalian species. *J. Physiol (London)*. **158**, 1-14.
- Farmer, C.G.** (2015). The evolution of unidirectional pulmonary airflow. *Physiology* **30**, 260-272.
- Farmer, C.G., and Carrier, D.R.** (2000). Pelvic aspiration in the American alligator (*Alligator mississippiensis*). *J. Exp. Biol.* **203**, 1679-1687.
- Gans, C., and Clark, B.** (1976). Studies on ventilation of *Caiman crocodilus* (Crocodilia: Reptilia). *Respiration Physiology*. **26**, 285-301.
- Gaunt, A.S., and Gans, C.** (1969). Mechanics of respiration in the snapping turtle, *Chelydra serpentina* (Linné). *J. Morphol.* **128**, 195-228.
- Hong, S.K., Cerretelli, P., Cruz, J.C., and Rahn, H.** (1969). Mechanics of respiration during submersion in water. *Journal of Applied Physiology*. **27**, 535-538.
- Jackson, D.C.** (1971). Mechanical basis for lung volume variability in the turtle *Pseudemys scripta elegans*. *Am. J. Physiol.* **220**, 754-758.
- Klein, W., Owerkowicz, T.** (2006). Function of intracoelomic septa in lung ventilation of Amniotes: Lessons from lizards. *Physiol. Biochem. Zool.* **79**, 1019-1032

Klein, W., Abe, A.S., Perry, S.F. (2003). Static lung compliance and body pressures in *Tupinambis merianae* with and without post-hepatic septum. *Respi. Physiol.* **135**, 73-86.

Lutcavage, M.E., Lutz, P.L., and Baier, H. (1989). Respiratory mechanics of the loggerhead sea turtle, *Caretta caretta*. *Respiratory Physiology.* **76**, 13-24.

Milsom, W.K., and Vitalis, T.Z. (1984). Pulmonary mechanics and the work of breathing in the lizard, *Gekko gecko*. *J. Exp. Biol.* **113**, 187-202.

Munns, S.L., Evans, B.K. and Frappell, P.B. (1998). The effect of environmental temperature, hyp[oxia, and hypercapnia on the breathing patterns of saltwater crocodiles (*Crocodylus porosus*). *Physiol. Zool.* **71**, 267-273.

Munns, S.L., Owerkowicz, T., Andrewartha, S.J., Frappell, P.B. (2012). The accessory role of the diaphragmaticus muscle in lung ventilation in the estuarine crocodile *Crocodylus porosus*. *J. Exp. Biol.* **215**, 845-852.

Naifeh, K.H., Huggins, S.E., Hoff, H.E., Hugg, T.W. and Norton, R.E. (1970). Respiratory patterns in crocodylian reptiles. *Respir. Physiol.* **9**, 31-42.

Otis, A. B., Fenn, W. O. and Rahn, H. (1950). Mechanics of breathing in man. *J. Appl. Physiol.* **2**, 592-607.

Perry, S.F. (1988). Functional morphology of the lungs of the Nile crocodile, *Crocodylus niloticus*: non-respiratory parameters. *J. Exp. Biol.* **134**, 99-117.

Perry SF. (1998). Lungs: comparative anatomy, functional morphology, and evolution. In: *Biology of the Reptilia*, vol **19** (Gans C, Gaunt AS, eds), pp 1-92, Ithaca, New York.

Perry, S.F. and Duncker, H. R. (1978). Lung architecture, volume and static mechanics in five species of lizards. *Respir. Physiol.* **34**, 61-81.

Perry S.F., Codd, J.R. and Klein, W. (2005). Evolutionary biology of aspiration breathing and origin of the mammalian diaphragm. *Rev. Mal. Respir.* **22**, 2519-2538

Rosenberg, I. (1973). Functional anatomy of pulmonary ventilation in the garter snake, *Thamnophis elegans*. *J. Morphol.* **140**, 171 - 184.

Sanders, R.K. and Farmer, C.G. (2012). The pulmonary anatomy of *Alligator mississippiensis* and its similarity to the avian respiratory system. *Anat. Rec.* **295**, 699-714.

Tattersall, G.J., Andrade, D.V., Brito, S.P., Abe, A.S. and Milsom, W.K. (2006) Regulation of ventilation in the caiman (*Caiman latirostris*): effects of inspired CO₂ on pulmonary and upper airway chemoreceptors. *J. Comp. Physiol. B.* **176**, 125-138.

Uriona, T.J., Farmer, C.G. (2006) Contribution of the diaphragmaticus muscle to vital capacity in fasting and post-prandial American alligators (*Alligator mississippiensis*). *J. Exp. Biol.* **209**, 4313-4318.

Uriona, T.J., Farmer, C.G. (2008). Recruitment of the diaphragmaticus, ischiopubis and other respiratory muscles to control pitch and roll in the American alligator (*Alligator mississippiensis*). *J. Exp. Biol.* **211**, 1141-1147.

Uriona, T.J., Lyon, M., Farmer, C.G. (2009). The importance of the M. diaphragmaticus to the duration of dives in the American alligator (*Alligator mississippiensis*). *Zoology* **112**, 263-169.

Vickaryous, M.K., Hall, B.K. (2008). Development of the dermal skeleton in *Alligator mississippiensis* (Archosauria, Crocodylia) with comments on the homology of osteoderms. *J. Morph.* **269**, 398-422.

Vitalis, T. A. and Milsom, W. K. (1986). Pulmonary mechanics and the work of breathing in the semi-aquatic turtle *Pseudemys scripta*. *J. Exp. Biol.* **125**, 137-155.

Tables

Table 1; Static body wall compliance (C_B), lung compliance (C_L), and total compliance (C_T) of various species of reptiles and mammals. Species are listed in descending order of C_T . Compliance values as ml/cm H₂O/kg

Species	Wt (kg)	C_T	C_L	C_B	Reference
Chameleon <i>Chamaeleo chamaeleon</i>	0.019	306	759	512	Perry and Duncker, 1978
Savana Monitor <i>Varanus exanthematicus</i>	0.249	67	365	82	Perry and Duncker, 1978
Tokay Gecko <i>Gekko gekko</i>	0.108	47	273	57	Perry and Duncker, 1978
Juvenile Caiman <i>Caiman yacare</i>	0.039	28.9	154	33.9	This study
Tegu Lizard <i>Tupinambis merianae</i>	0.707	23.1	90.7	39.7	Klein et al., 2003
Green Lizard <i>Lacerta viridis</i>	0.028	18	62	27	Perry and Duncker, 1978
Tokay Gecko <i>Gekko gekko</i>	0.108	16	202	15	Milsom and Vitalis, 1984
Nile Crocodile <i>Crocodylus niloticus</i>	4.11	12.3	73.9	10.6*	Perry, 1988
Adult Caiman <i>Caiman yacare</i>	27.9	12.0	42.5	16.7	This study
Red Eared Slider <i>Pseudemys scripta</i>	0.250- 0.600	10	170	11	Jackson, 1971
Red Eared Slider <i>Pseudemys scripta</i>	0.726	8	35	12	Vitalis and Milsom, 1986
Dog	12.6	2.1	3.17	2.54	Crossfill and Widdicombe, 1961
Rat	0.250	1.24	1.56	5.88	Crossfill and Widdicombe, 1961
Human	70	1.48	2.9	3.0	Crossfill and Widdicombe, 1961

Table 2; Static body wall compliance (C_B), lung compliance (C_L), and total compliance (C_T) of various species of reptiles and mammals. Species are listed in descending order of C_T . Compliance values in ml/cm H₂O/ml V_{LR}

Species	V_{LR} ml/kg	V_L ml/kg	C_T	C_L	C_B	Reference
Chameleon <i>Chamaeleo chamaeleon</i>	231	1158	2.50	5.73	3.84	Perry and Duncker, 1978
Tokay Gecko <i>Gekko gekko</i>	65	307	0.73	4.22	0.89	Perry and Duncker, 1978
Nile Crocodile <i>Crocodylus niloticus</i>	18	109.4	0.71	4.32	0.85	Perry, 1988
Adult Caiman <i>Caiman yacare</i>	17.9	142.8	0.67	2.38	0.93	This study
Savana Monitor <i>Varanus exanthematicus</i>	122	510	0.66	3.27	0.83	Perry and Duncker, 1978
Tegu Lizard <i>Tupinambis merianae</i>	34.1	173	0.55	1.3	1.09	Klein et al., 2003
Green Lizard <i>Lacerta viridis</i>	46	189	0.53	1.78	0.76	Perry and Duncker, 1978
Juvenile Caiman <i>Caiman yacare</i>	66.7	185.9	0.44	2.37	0.52	This study
Tokay Gecko <i>Gekko gekko</i>	65	347	0.25	3.17	0.23	Milsom and Vitalis, 1984
Red Eared Slider <i>Pseudemys scripta</i>	110		0.10	1.70	0.11	Jackson, 1971
Rat	6		0.10	0.12	0.55	Crossfill and Widdicombe, 1961
Red Eared Slider <i>Pseudemys scripta</i>	16	262	0.08	0.35	0.12	Vitalis and Milsom, 1986
Dog	20		0.054	0.12	0.098	Crossfill and Widdicombe, 1961
Human	29		0.034	0.066	0.068	Crossfill and Widdicombe, 1961

Figures

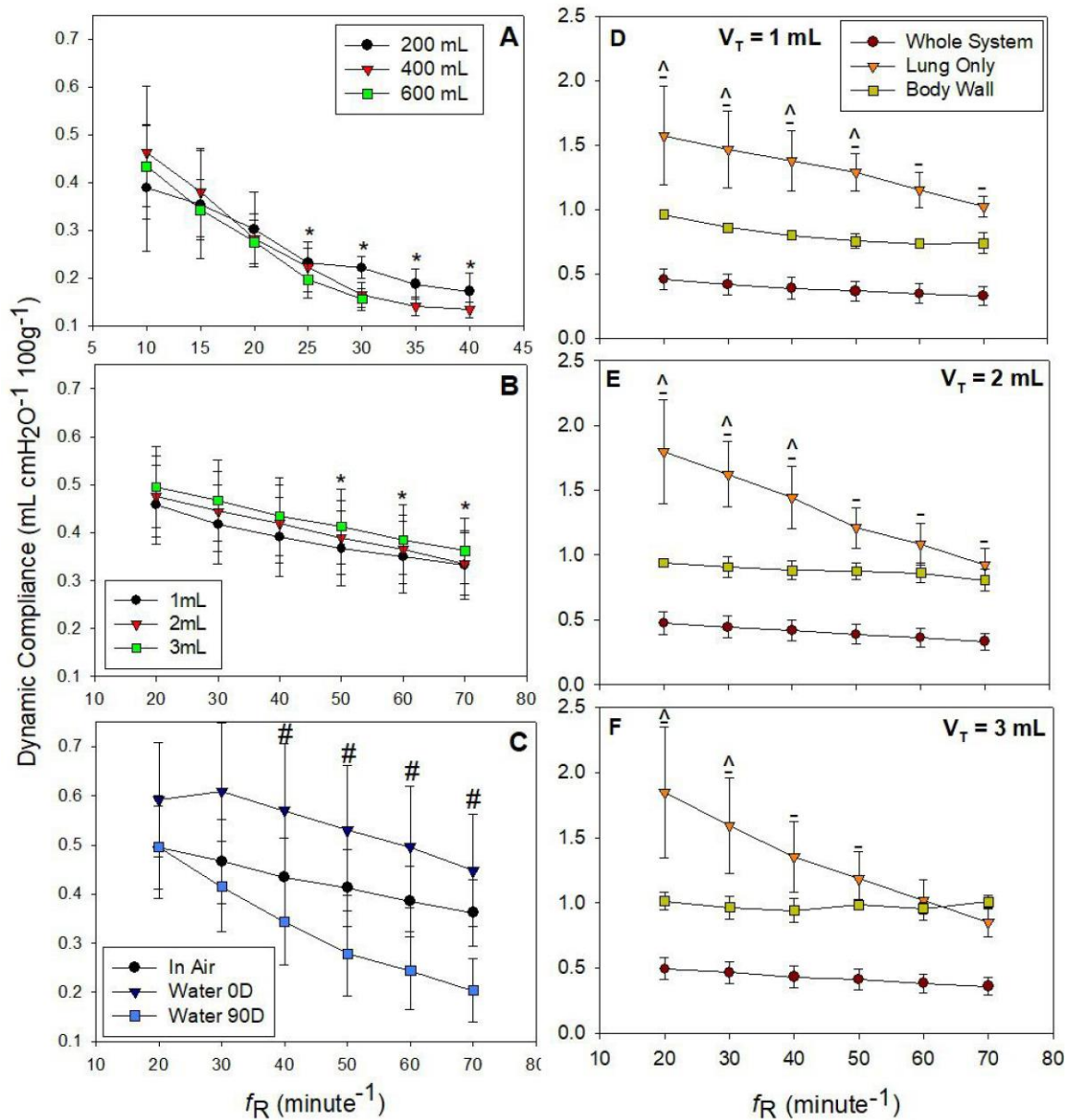


Figure 1: Comparison of adult (A) and juvenile (B) total system dynamic compliance (C_T) at all combinations of f_R and V_T tested. * indicates a significant difference between 10 breaths/minute and the indicated f_R (for all V_T at that f_R). C illustrates the effect of water submergence on dynamic compliance for juvenile caiman at a V_T of 3 mL. Significant differences between dynamic compliance at 0°D and 90°D are indicated by #. D, E, and F illustrate changes in C_T , lung only, and the body wall of juvenile caiman as f_R is increased for a given V_T (D = 1 mL, E = 2 mL, F = 3 mL). ^ indicates significant differences between the whole system and the lung only and ^ indicates a significant difference between the lung only and the body wall. Data are means ($N = 4$ for adults, $N = 5$ for juveniles) ± 1 SEM.

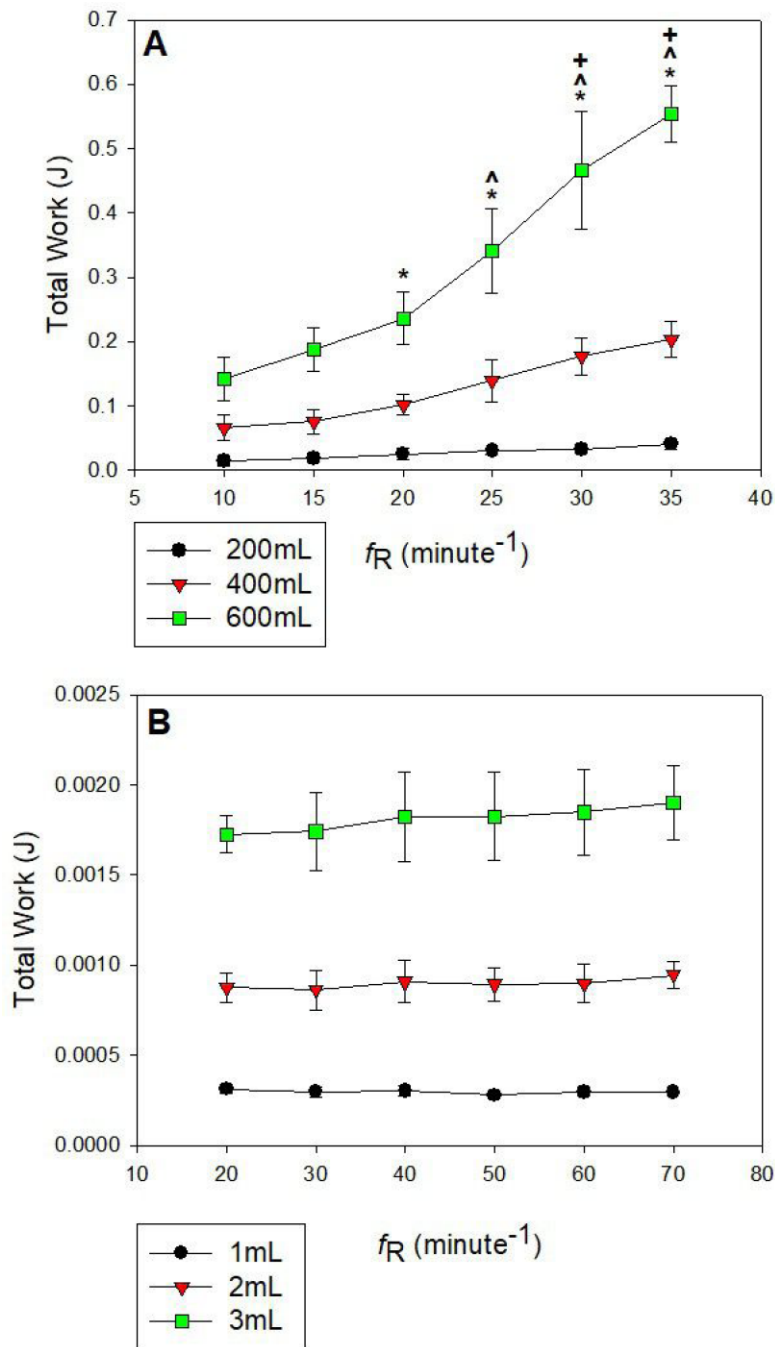


Figure 2: Total work required to ventilate adult (A) and juvenile (B) intact respiratory systems across a range of f_R and V_T . Note the large difference in y-axis scaling. Symbols indicate significant difference in total work compared to 10/min within $V_T = 600\text{mL}$ (*), 400mL (^), and 200mL (+). Total work is significantly different compared across all tidal volumes. Data are means ($N = 4$ for adults, $N = 5$ for juveniles) ± 1 SEM.

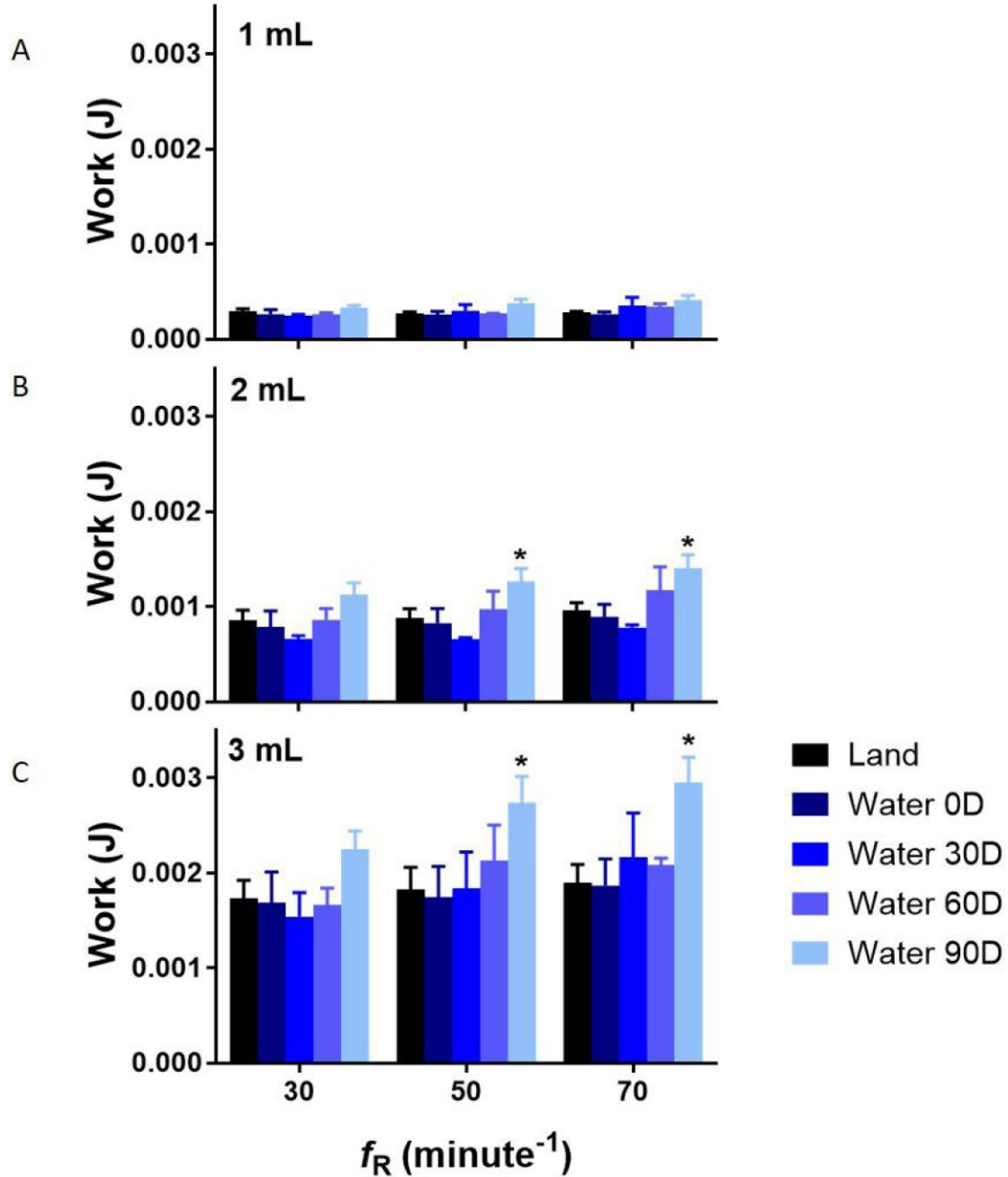


Figure 3: Comparison of total work of breathing in juvenile caiman lying on land and in water at angles of 0°, 30°, 60°, and 90° to the water surface at $V_T = 1$ (A), 2 (B), and 3 mL (C) and $f_R = 30, 50, 70$ breaths/minute. * indicates a significant difference in the work required to breathe at 90° compared to all other conditions.

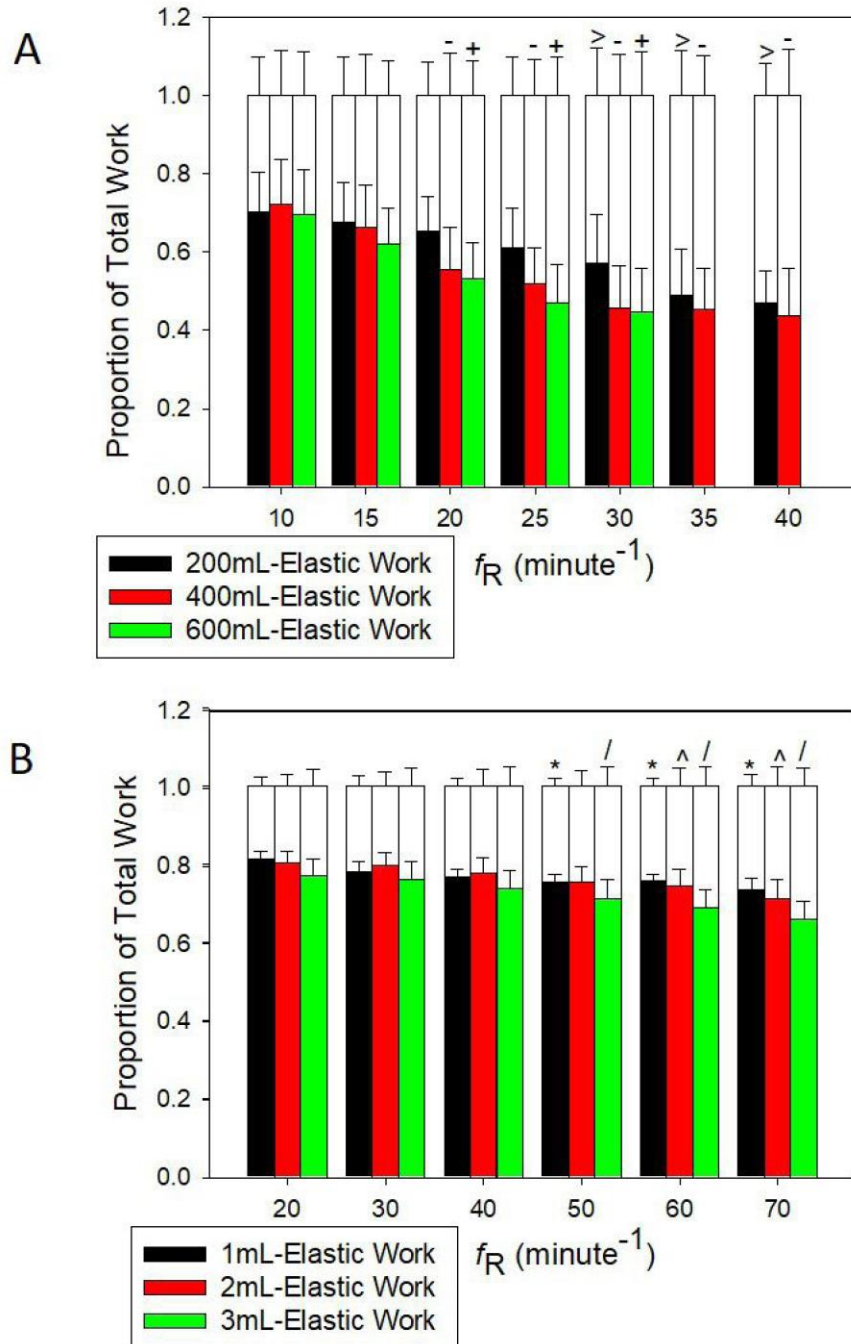


Figure 4: Proportion of total work required to overcome resistive forces (open bars) and elastic forces (coloured bars) at different V_T and f_R in adults (A) and juvenile caiman (B). Symbols indicate significant differences compared to 10 breaths/min within 200mL (>), 400 (-), or 600 (+) or to 20 breaths/minute within 1mL (*), 2mL (^), or 3mL (/). Data are means ($N = 4$ for adults, $N = 5$ for juveniles) ± 1 SEM.

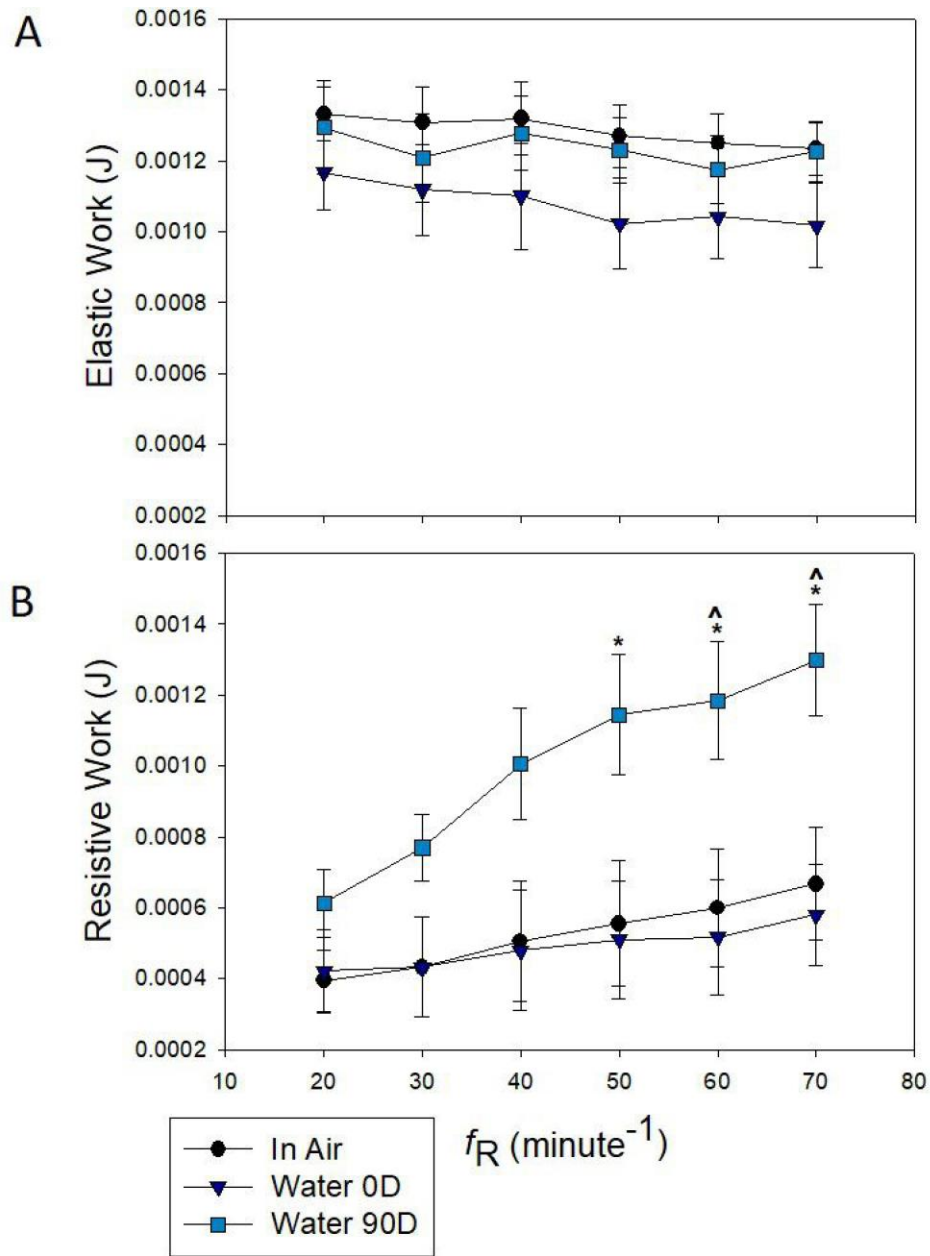


Figure 5: Work required to overcome elastic (A) and resistive forces (B) in animals lying on land and in water at angles of 0° and 90° to the water surface at a tidal volume of 3 mL. Symbols indicate significant differences between work at 90° submergence and 0° (*) or 90° submergence and in air (^). Data are means (N = 5) ± 1 SEM.

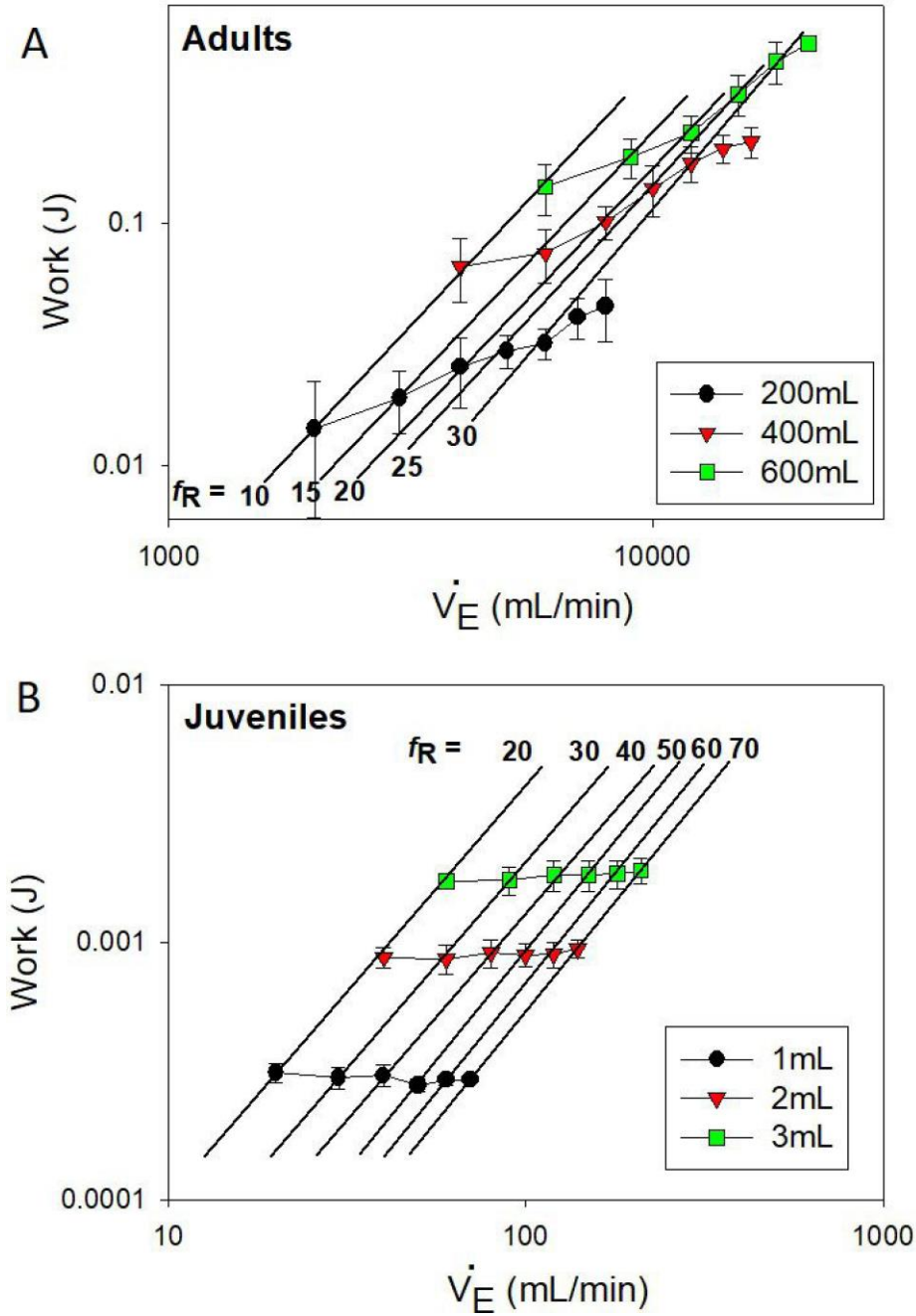


Figure 6: The relationship between total work and minute ventilation for adult (A) and juvenile (B) caiman at different combinations of V_T (symbols and horizontal lines) and f_R (represented as vertical isopleths). Data are means ($N = 4$ for adults, $N = 5$ for juveniles) ± 1 SEM.

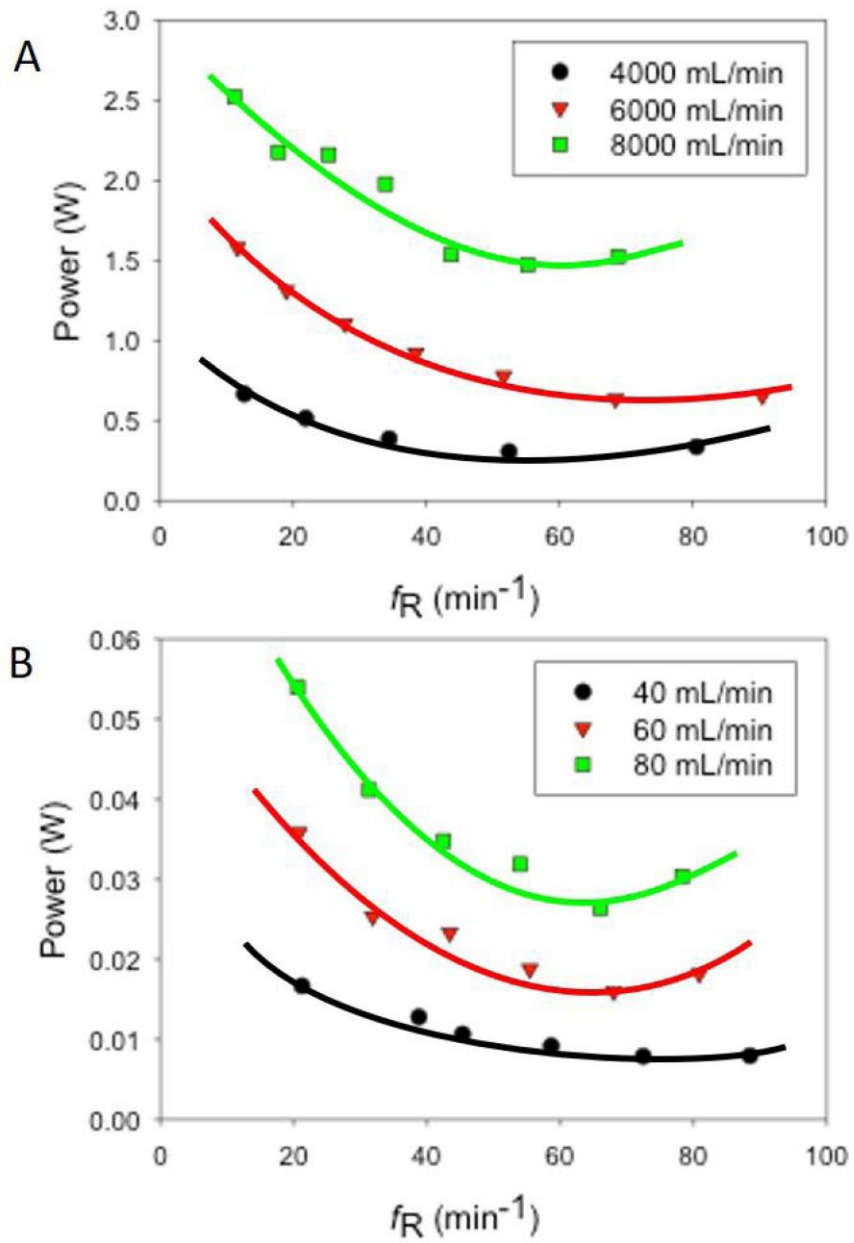


Figure 7: Relationship between power and f_R for three levels of minute ventilation in adults (A) and juveniles (B). Data are derived from Figure 8, as described in the text.

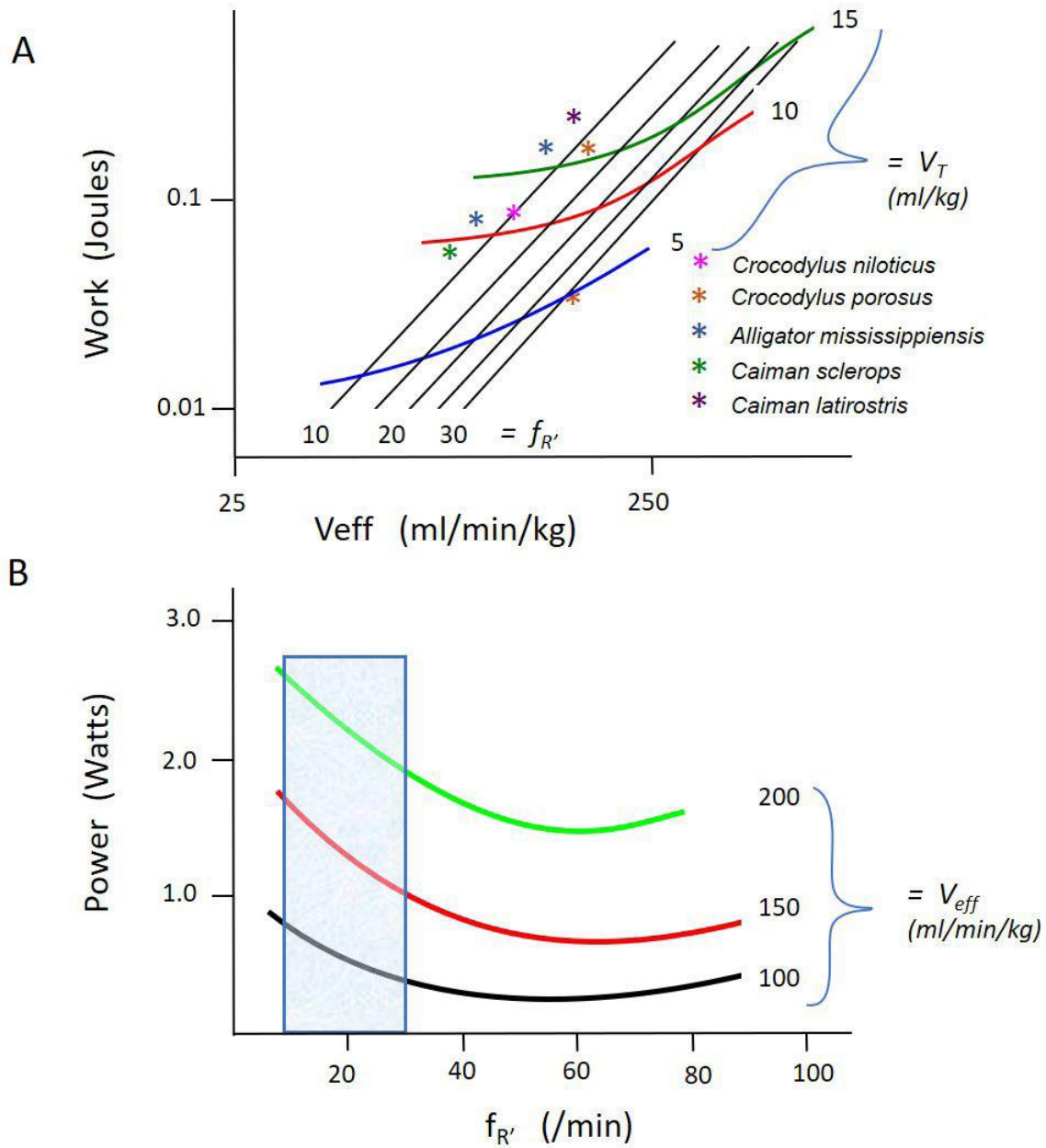


Figure 8. A. The mechanical cost (work in Joules) required to produce single breaths at various levels of V_T as a function of instantaneous frequency ($f_{R'} = 60/T_{TOT}$). The values of V_T and $f_{R'}$ for intact crocodilians spontaneously breathing various gas mixtures (Table 4) are placed on the graph for comparison. B. The power required to maintain different constant levels of alveolar ventilation are plotted as a function of pump frequency ($f_{R'}$). The range of combinations of $f_{R'}$ and V_T measured in different species of spontaneously breathing crocodilians is superimposed on these curves as a shaded box.

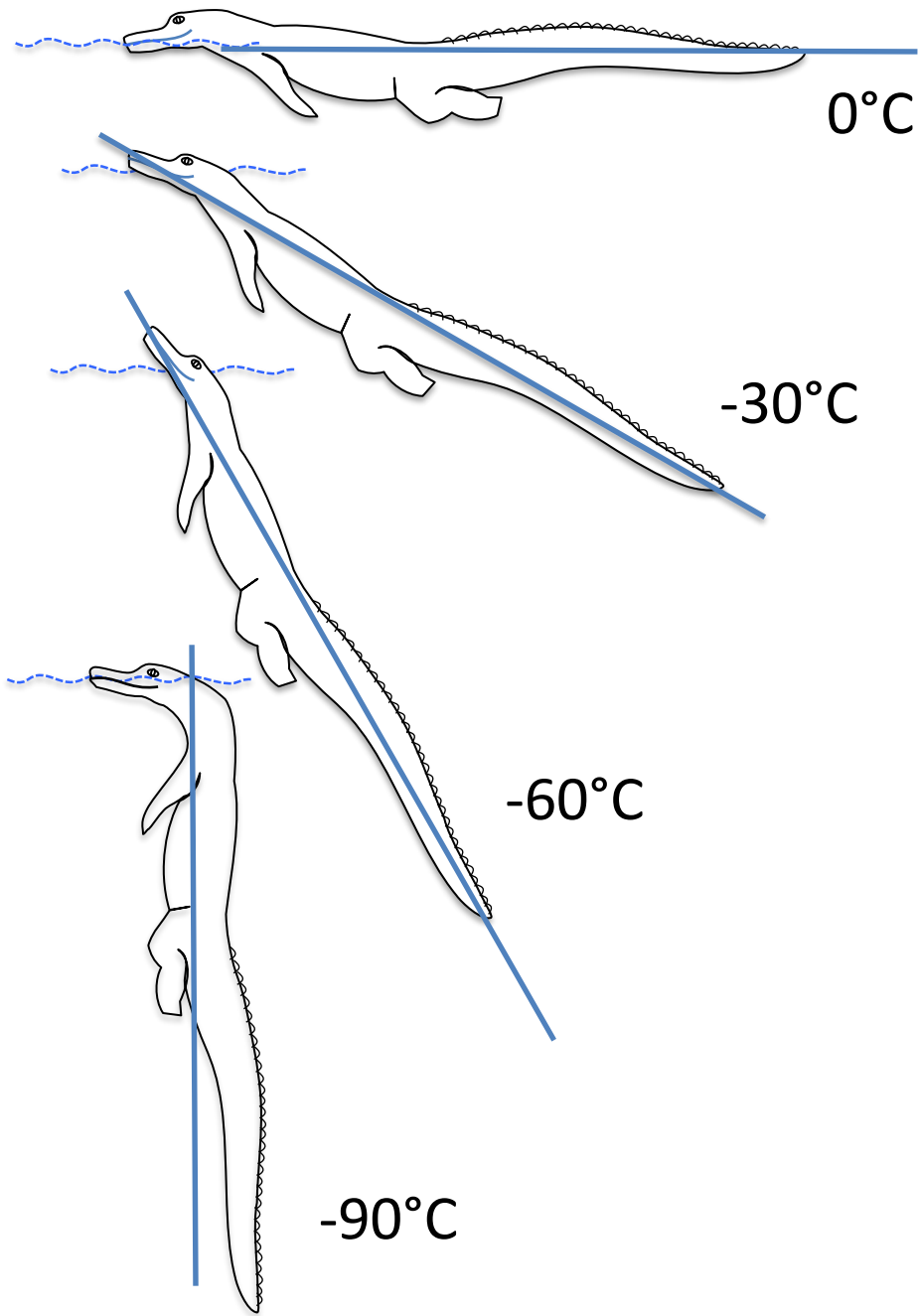


Figure S1. Schematic diagram illustrating the position of the juvenile caiman within the water column. Angles are in relation to the surface of the water.

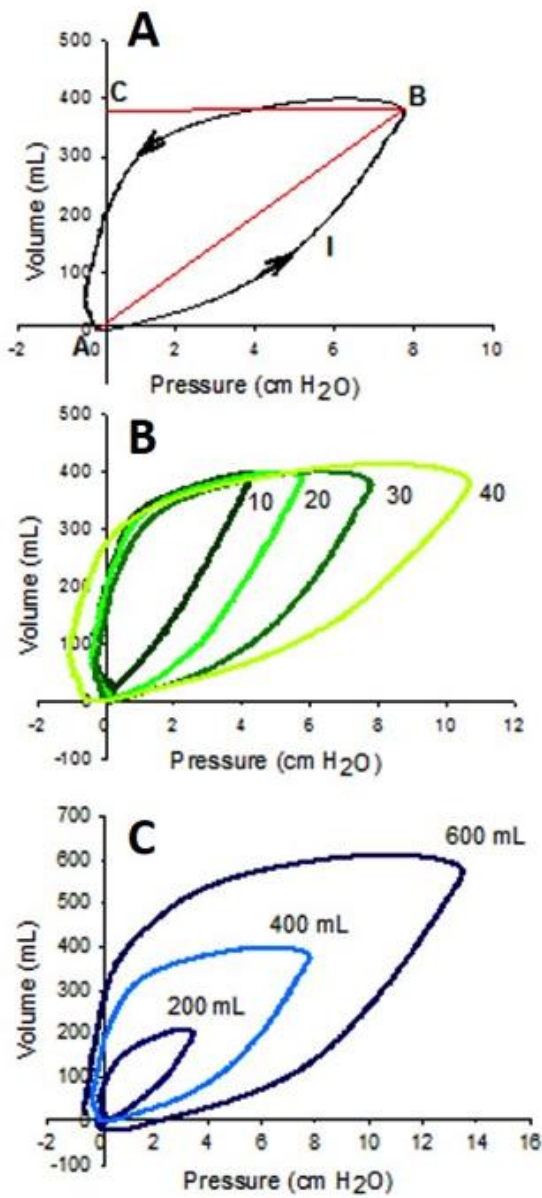


Figure S2. Schematic diagrams of the pressure-volume relationships during a ventilator cycle of an intact respiratory system. A illustrates the areas of the curve used for work calculations (see text for explanation). B and C illustrate the effect of increasing f_R and V_T , respectively, on intratracheal pressure.

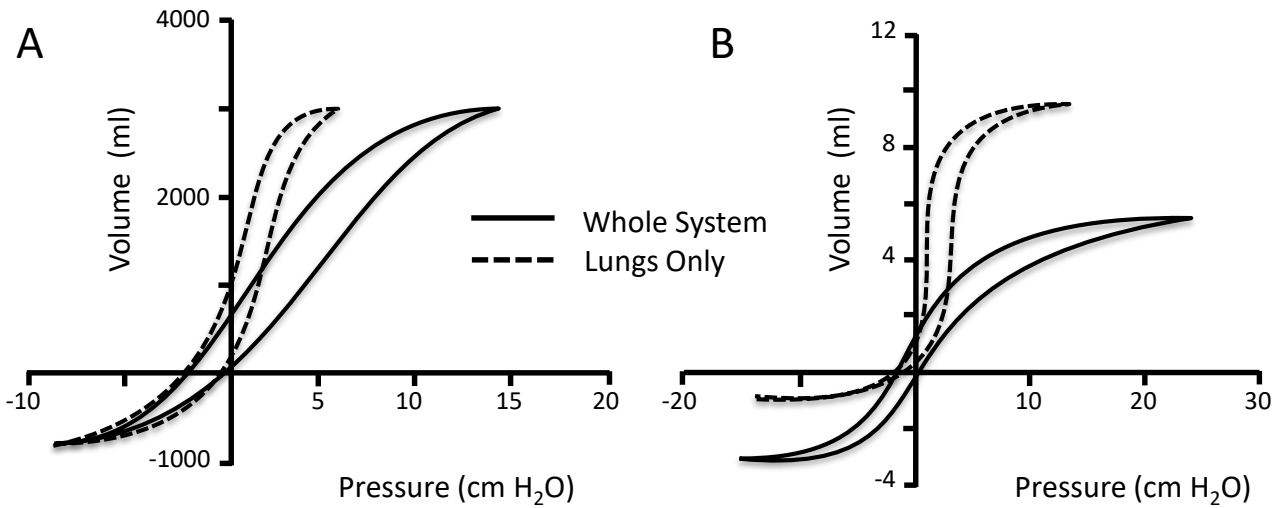


Figure S3. Static Pressure-volume curves of the intact system (solid lines) and the isolated lungs (broken lines) in adult (A) and juvenile (B) caiman.



Figure S4. Photos of juvenile caiman floating with their bodies at different angles to the water surface.

		Weight kg	Temperature	VT ml/kg	$f_{R'}$ /min
Munns et al, 2012	<i>Crocodylus porosus</i>	0.98	30	16	11
Munns et al 1998	<i>Crocodylus porosus</i>	0.2 - 0.6	28-30	20	31
Farmer and Carrier 2000	<i>Alligator mississippiensis</i>	1.34	30	22	7
Naifeh et al., 1970	<i>Caiman sclerops</i>	0.68	23-25	12.2	8
	<i>Alligator mississippiensis</i>	0.72	23-25	7.8	7
Tattersall et al 2006	<i>Caiman latirostris</i>	1.56	25	9.3	8
Glass and Johansen 1979	<i>Crocodylus niloticus</i>	5.0	25	11	10

Table S1. Tidal volume and instantaneous breathing frequencies of various crocodylian species taken from the literature



Figure S5. Thermal panting (gular flutter) in a crocodilian